Materials Science & Engineering C 118 (2021) 111514

Contents lists available at ScienceDirect

Materials Science & Engineering C

journal homepage: www.elsevier.com/locate/msec

Electrospun formulation of acyclovir/cyclodextrin nanofibers for fast-dissolving antiviral drug delivery

Asli Celebioglu*, Tamer Uyar*

Department of Fiber Science & Apparel Design, College of Human Ecology, Cornell University, Ithaca, NY 14853, USA

ARTICLE INFO

Keywords:
Acyclovir
Hydroxypropyl-beta-cyclodextrin
Inclusion complex
Nanofibers
Electrospinning
Fast-dissolving drug delivery

ABSTRACT

Acyclovir is an effective antiviral drug which suffers from limited water solubility and low bioavailability. However, it is possible to eliminate these limitations by forming inclusion complexes with cyclodextrins. In this study, we have reported the electrospinning of polymer-free and free-standing acyclovir/cyclodextrin nanofibers for the first time. This is a promising approach for developing a fast-dissolving delivery system of an antiviral drug molecule. Here, hydroxypropyl-beta-cyclodextrin (HP-βCD) was used as both complexation agent and electrospinning matrix. The acyclovir/HP-βCD system was prepared by incorporating ~7% (*w*/w) of acyclovir into the highly concentrated aqueous solution of HP-βCD (180%, *w*/*v*). The control sample of acyclovir/polyvinylpyrrolidone (PVP) nanofiber were also generated using ethanol/water (3/1, *v*/v) solvent system and the same initial acyclovir (7%, *w*/w) content. Due to the inclusion complexation, acyclovir/HP-βCD nanofibers provided better encapsulation and so loading efficiency. The loading efficiency of acyclovir/HP-βCD nanofibers was determined as ~98%, while it was ~66% for acyclovir/PVP nanofibers. It was found that acyclovir/HP-βCD nanofibers contained some crystalline form of acyclovir. Even so, it showed faster dissolving/release and faster disintegration profiles compared to acyclovir/PVP nanofibers which had higher amount of crystalline acyclovir. The inclusion complexation property and high water solubility of HP-βCD (> 2000 mg/mL) ensured the fast-dissolving property of acyclovir/HP-βCD nanofibers. Briefly, acyclovir/HP-βCD nanofibers are quite promising alternative to the polymeric based system for the purpose of fast-dissolving oral drug delivery. The enhanced physicochemical properties of drug molecules and the use of water during whole process can make drug/cyclodextrin nanofibers a favorable dosage formulation for the desired treatments.

1. Introduction

The current developments in the fast-dissolving oral drug delivery system has been followed with a great interest in the pharmaceutical industry [1,2]. For fast-dissolving systems, the contact of product with saliva is enough to be dissolved and/or disintegrated in the oral cavity. Therefore, there is no need for an additional use of water or chewing process differently from conventional drug formulation. The fast-dissolving oral delivery system can eliminate the disadvantages of poorly water-soluble drugs by improving their solubility, bioavailability and delivery [1,2]. The fast-dissolving oral delivery system might be essential for children to elderly who have troubles such as swallowing, chewing, or vomiting during applications [1–3]. The bedridden patients, travelers, and the one who is getting local treatments (oral ulcer, toothaches, or herpes *etc*.) can also take advantages of the fast-dissolving systems [1–3]. The unpleasant mouthfeel might also be a concern for these patients when large grains of drug are quite slowly disappeared by the saliva.

Fast-dissolving systems can be in the different forms such as films/strips [1,2], patches/wafers [4], tablets [5], or capsules [6]. All these formulations can be produced by using various approaches including extrusion, solvent casting, spraying, tableting, lyophilization [1–6]. Recently, nanotechnological methods has been also adopted for developing fast-dissolving delivery systems. The electrospinning is one of these methods which enables to fabricate free-standing webs composed of nano-sized fibrous structures. The electrospinning is an adaptable electrohyrodynamic atomization technique which enables to produce electrospun nanofibers loaded with drug molecules [7–9]. The incorporation of drug molecules within the electrospun nanofibers can be also performed in different ways using the various modified version of electrospinning such as coaxial [10], triaxial [11], Janus [12] and sheath-separate-core [13] systems. Due to drug carrier and delivery potential, high surface area and 3D porous structure, electrospun nanofibers has become attractive for fast-dissolving oral drug delivery

* Corresponding authors.
E-mail addresses: ac2873@cornell.edu (A. Celebioglu), tu46@cornell.edu (T. Uyar).

https://doi.org/10.1016/j.msec.2020.111514
Received 24 July 2020; Received in revised form 24 August 2020; Accepted 4 September 2020
Available online 16 September 2020
0928-4931/

purposes [7,8]. In other words, the nanofibrous webs can ensure a faster absorption of drug molecules than the conventional formulation owing to their unique properties. Moreover, they can resolve the unpleasant granular feeling arising with the drug applications.

The electrospun nanofibrous webs of hydrophilic polymers can be functionalized with variety of drugs and emerged as a fast-dissolving oral delivery system by enhancing the water solubility of the drug molecules [14–18]. It has been reported that, several polymer types including polyvinylpyrrolidone (PVP) [14–16,19–21], poly(vinyl alcohol) (PVA) [17], gelatin [22], Eudragit [23] *etc*. have been used in order to develop fast-dissolving drug delivery systems in the form of electrospun nanofibers. It is worthy to mention that PVP has been already used as polymeric surfactant for dispersing the poorly soluble active pharmaceutical ingredient (API) in the formulation of pharmaceutical tablets [24,25]. This might make PVP to be the most frequently reported polymer types among others for the electrospinning of fast-dissolving nanofibers [24,25].

The fast-dissolving nanofibrous webs of PVP have been fabricated by the incorporation of poorly water-soluble drugs of aceclofenac [14], ornidazole [15], amlodipine besylate/valsartan [16], loratadine [19], isosorbide dinitrate [20] and mebeverine [21]. In all these studies, non-aqueous solvent systems have been used to dissolve both PVP and drug molecules and for the further electrospinning process. Here, the fast evaporation of these solvents has hindered the re-crystallization of drug molecules during the electrospinning and has provided amorphous distribution through the nanofibrous webs [7,8]. The amorphous state of drug molecules in the formulation is desirable for fast-dissolving feature, however the use of organic and toxic solvents might be concerned from the point of production and administration of these dosage forms. On the other hand, cyclodextrin molecules has turned out to be an attractive alternative by eliminating most of the concerns arising with the use of polymeric systems.

As a type of oligosaccharides, cyclodextrins (CDs) has a growing contribution in the scientific research and the worldwide market of pharmaceuticals [26–30]. The main source of interest in the use of CDs is due to their unique property of non-covalent inclusion complexation which can offer an enhanced solubility, stability and bioavailability for API in the dosage formulations [26,27,31]. In addition to these, different release profiles (fast, sustained or controlled), masking of the unpleasant taste and preventing of the tissue irritation are the other advantages which can be provided by the use of CD inclusion complexes [26,27,31]. The CD inclusion complexes make difference particularly in terms of aqueous solubility which can also ensure an enhanced bioavailability for the poorly soluble drugs [26,27,31,32]. There are recent reports in the literature describing the potential of CD inclusion complex incorporated polymer-based nanofibers for fast-dissolving drug delivery system [33,34].

As it has been recently shown by both our and other groups, it is also possible to develop polymer free CD inclusion complex nanofibers from variety of drug types including antibiotic (sulfisoxazole [35], metronidazole [36]), pain reliever/fever reducer (paracetamol [37], diclofenac sodium [38]), anti-inflammatory (ibuprofen [39], hydrocortisone [40]), antifungal (voriconazole [41]) and diuretic (spironolactone [42]). The fast-dissolving drug delivery system based on CD inclusion complex nanofibers might be a promising alternative to the polymeric systems due to the complexation property of CD which can provide concurrent enhancement for drug solubility and bioavailability [26,31]. It is noteworthy to mention that CD inclusion complex nanofibers have been fabricated in aqueous system and an additional organic solvent system has not been used to dissolve drug molecules which might be a common case for polymeric nanofibers.

Acyclovir (9-(2-Hydroxyethoxymethyl)guanine) is one of the most effective antiviral drug used for the selective treatment of herpes simplex virus (HSV-1/2) and varicella zoster [43,44]. The administration of acyclovir includes the topical, oral, and parenteral treatments. However, poor physicochemical properties including limited aqueous solubility, bioavailability and membrane permeability decrease the therapeutic potential of acyclovir [43,44]. The low bioavailability (15–30%) and low permeability of acyclovir can cause slow, incomplete and highly variable absorption profile especially in case of oral therapy [43]. Since the aqueous solubility is the key factor for improving both bioavailability and absorption of drugs, there has been remarkable effort to enhance the therapeutic efficiency of acyclovir, as well [43,45]. The different carrier and delivery systems such as liposomes, micro/nanoparticles, microemulsions *etc*. have been investigated in order to improve the solubility and the oral bioavailability of acyclovir [43,45]. Additionally, various native and modified CD types have been applied for improving the solubility and delivery of acyclovir by forming inclusion complexes [45–50]. The inclusion complexation with CD has provided an enhanced physicochemical property for acyclovir molecule and hydroxypropyl-beta-cyclodextrin (HP-βCD) has become prominent among other CD types [45,51]. Even, in one of the related reports, Nair et al. demonstrated the bioavailability of acyclovir/HP-βCD system for the oral therapy by *in vivo* studies [45]. This is most probably due to the exceptional properties such as high water solubility, non-toxicity and stability of HP-βCD which have been also reported in previous studies dictated its widespread use in pharmaceutical areas [45,52–54].

The acyclovir incorporated electrospun nanofibers have been fabricated using hydrophobic [55–57], hydrophilic [58], or blend polymer matrix [59,60]. Even, the potential of acyclovir incorporated nanofibers has been shown for ocular delivery [61], topical delivery [44] and HSV-2 treatments [62]. The fast-dissolving oral delivery system of acyclovir nanofibers might be one of the emerged treatment types of this antiviral drug and might be a feasible alternative to the conventional dosage formulation. For this purpose, we have fabricated the acyclovir/HP-βCD inclusion complexes in the form of polymer-free electrospun nanofibers for the first time (Fig. 1). The control nanofibrous web has been obtained from one of the most commercially used hydrophilic polymer type of PVP. The further characterization of these two nanofibrous webs have been carried out to demonstrate their structural properties and dissolution/release profiles.

2. Experimental procedures

2.1. Materials

Hydroxypropyl-beta-cyclodextrin (HP-βCD) (Cavasol W7 HP, DS: ~ 0.9) was presented by Wacker Chemie AG (USA). The as received polyvinylpyrrolidone (PVP, Mw: 40 kDa, Sigma Aldrich), acyclovir (98.0%, TCI America), dimethyl sulfoxide (DMSO, > 99.9%, Sigma Aldrich), sodium chloride (NaCl, > 99%, Sigma Aldrich), o-phosphoric acid (85% (HPLC), potassium phosphate monobasic (KH_2PO_4, ≥ 99.0%, Fisher Chemical), sodium phosphate dibasic heptahydrate (Na_2HPO_4, 98.0–102.0%, Fisher Chemical), Fisher Chemical) and deuterated dimethylsulfoxide (*d6*-DMSO, 99.8%, Cambridge Isotope) were supplied commercially. The high-quality water was distilled by Millipore Milli-Q ultrapure water system (Millipore, USA).

2.2. Electrospinning

The clear solutions of HP-βCD and PVP were prepared by the solid concentration of 180% (*w/v*) and 50% (w/v) in water and ethanol/water (3/1, *v*/v) solvent systems, respectively. Afterwards, acyclovir powder was added to HP-βCD and PVP solutions so as to provide ~7% drug content (*w*/w, in proportion to total sample amount). This acyclovir amount also corresponds to the molar ratio of 2/1 (CD/guest) in case of acyclovir/HP-βCD system. The acyclovir/HP-βCD and acyclovir/PVP solutions were stirred overnight at room temperature and turbid feature was observed for both systems. For control, the pure HP-βCD (200%, *w/v*) and PVP (50%, w/v) solutions were also prepared in the same solvent systems to produce pristine HP-βCD and PVP nanofibers. Prior the electrospinning, the solution properties of viscosity and

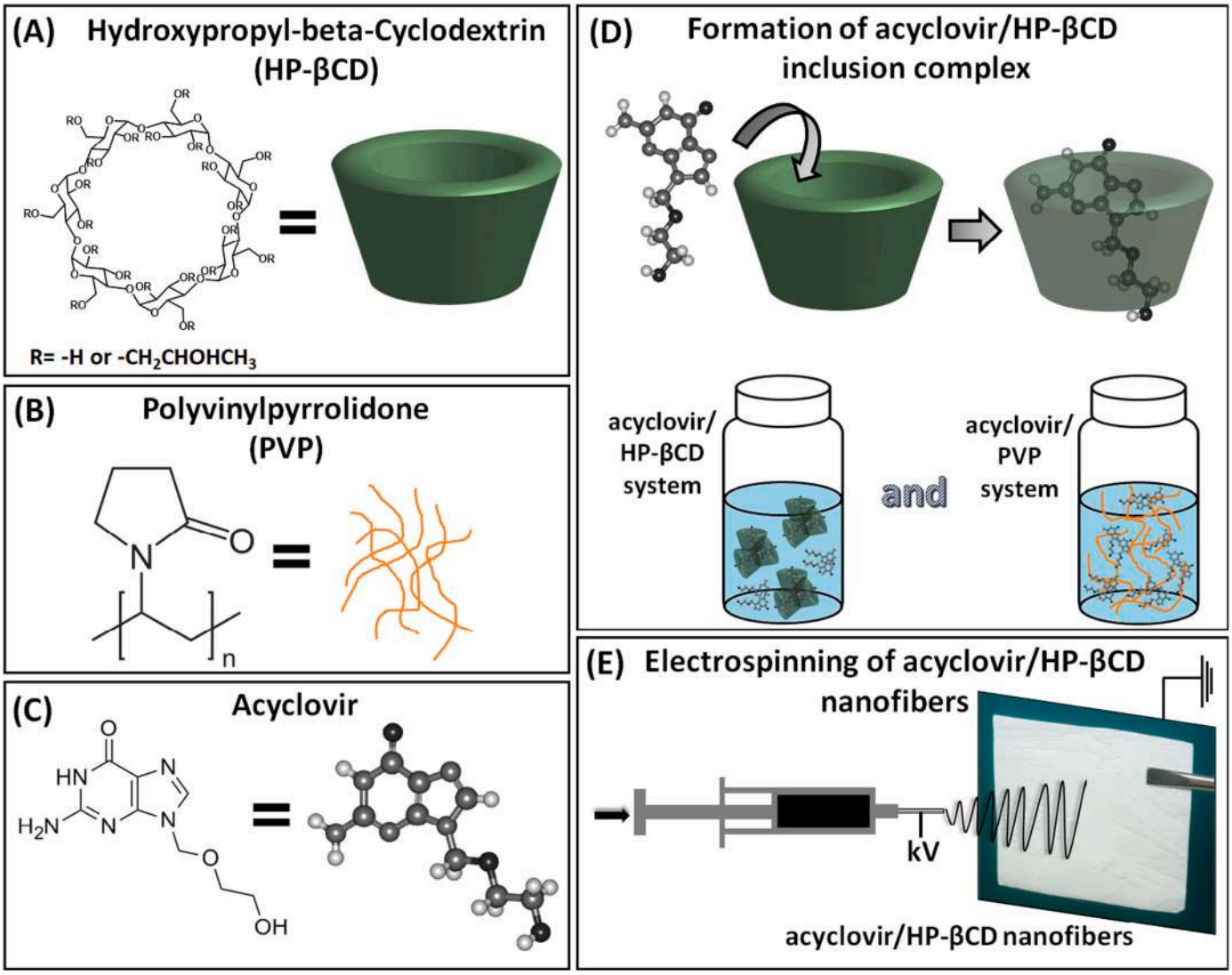

Fig. 1. The chemical structure of (A) HP-βCD, (B) PVP and (C) acyclovir. Schematic illustration of (D) the inclusion complex formation between acyclovir and HP-βCD molecules, and (E) the electrospinning of acyclovir/HP-βCD nanofibers.

conductivity were determined for each system using proper tools. The rheometer (AR 2000 rheometer, TA Instrument, USA) (20 mm cone/plate spindle (CP 20–4, 4°), shear rate range: 0.01–1000 s^{-1}, 21 °C) was used for the viscosity measurement, while the conductivity-meter (FiveEasy, Mettler Toledo, USA) was utilized for the conductivity measurements. The electrospinning equipment (Spingenix, model: SG100, Palo Alto, USA) was employed for the electrospinning of nanofibers. The acyclovir/HP-βCD and acyclovir/PVP systems were filled into the two separate plastic syringes (1 mL) which were fixated with metallic needles (21 or 23 G). The electrospinning solutions were fed through the tip of the needle by syringe pump with a stable flow rate (0.5 mL/h). Meanwhile, high voltage (15 kV) was applied to the needle and the nanofibers were concurrently collected on the grounded and steady metal plate which was placed at 15 cm from the needle and covered with Al foil. The ambient conditions of relative humidity and temperature were recorded to be 50% and 20 °C, respectively. It is noteworthy to mention that acyclovir/HP-βCD aqueous system had been initially prepared with 1/1 M ratio (14%, *w*/w), however electrospinning could not be conducted for this system because of its high turbidity and heterogeneity.

2.3. Phase solubility study

The phase solubility test was performed for acyclovir/HP-βCD system as reported previously [63]. The excess amount of acyclovir and HP-βCD with an increasing CD concentration from 0 to 160 mg/mL were mixed in 5 mL of water and shaken for 24 h on an incubator shaker (450 rpm, room temperature) by shielding from the light sources. Each incubated suspension was filtered using PTFE filter (0.45 μm) and UV–Vis-spectroscopy (PerkinElmer, Lambda 35, USA) (250 nm) was employed to measure the absorbance intensity of the filtered aliquots. The calibration curve ($R^2 \geq 0.99$) of acyclovir in water was used to convert the absorbance intensity to the concentration (mM) values. Triple experiment results (mean values ± standard deviations) were used to plot the phase solubility diagrams. The binding constants (K_s) were calculated from the equation; $K_s = slope/S_0(1\text{-}slope)$ where S_0 is the intrinsic solubility of acyclovir (~ 1.1 mg/mL).

2.4. Structural characterizations

The morphology of electrospun acyclovir/HP-βCD, HP-βCD, acyclovir/PVP and PVP nanofibers was determined using scanning electron microscope (SEM, Tescan MIRA3, Czech Republic) under high vacuum. To eliminate the charging problem, samples which were fixated on the

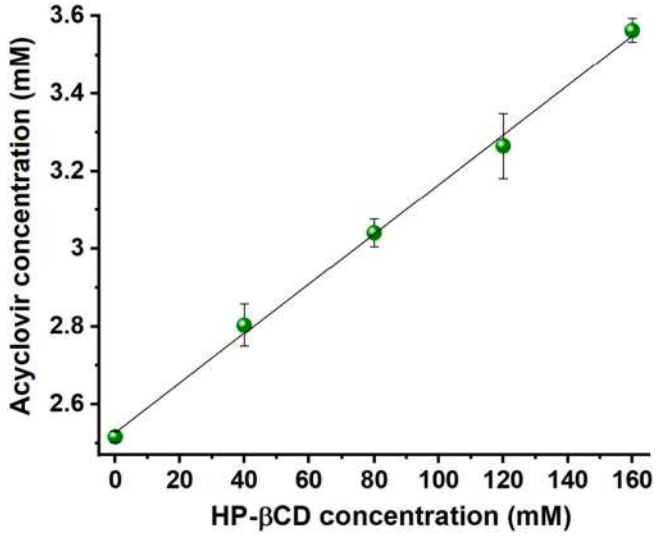

Fig. 2. Phase solubility diagram of acyclovir/HP-βCD system.

SEM stubs were sputtered with a thin layer of Au/Pd prior inserting into equipment. The SEM images were collecting by applying accelerating voltage of 10 kV with the working distance of 10 mm. ImageJ software was employed to calculate the average diameter (AD) (mean values ± standard deviations) of nanofibers (~100 fibers). Nuclear magnetic resonance spectrometer (Bruker AV500 having autosampler, USA) was used to prove the loading of acyclovir and to calculate the rough amount of acyclovir in acyclovir/HP-βCD and acyclovir/PVP nanofibers. For this, samples were initially dissolved in *d6*-DMSO with 40 mg/mL concentration and inserted into instrument to get proton nuclear magnetic resonance (^{1}H NMR) spectra (16 scan). The ^{1}H NMR spectra of samples were processed by using Mestranova software. The crystalline and the amorphous XRD pattern of acyclovir powder, acyclovir/HP-βCD, HP-βCD, acyclovir/PVP and PVP nanofibers were examined by using X-ray diffractometer (Bruker D8 Advance ECO, USA) (radiation source: Cu-Kα; 2θ region: 5°-30°; current/voltage: 25 mA/40 kV). The differential scanning calorimeter (DSC, Q2000, TA Instruments, USA) (temperature range: 0 °C - 280 °C; heating rate: 10 °C/min) and thermogravimetric analyzer (TGA, Q500, TA Instruments, USA) (temperature range: 25 °C - 600 °C; heating rate: 20 °C/min) were used in order to introduce the thermal profile of samples under inert atmosphere (N_2).

2.5. Loading efficiency test

For the calculation of loading efficiency, definite amount of acyclovir/HP-βCD and acyclovir/PVP nanofibers were dissolved in dimethyl sulfoxide (DMSO) and acyclovir content in these samples were determined by UV–Vis-spectroscopy (250 nm). The calibration curve of acyclovir in DMSO showed linearity and acceptability with $R^2 \geq 0.99$. The results were attained as mean values ± standard deviations by the triplicate experiments. The loading efficiency (%) was calculated using the equation; $Loading\ efficiency\ (\%) = Ce/Ct \times 100$ where Ce and Ct are the concentration of loaded acyclovir and the initial concentration of acyclovir, respectively.

2.6. In vitro release test

The time dependent *in vitro* release test of acyclovir/HP-βCD and acyclovir/PVP nanofibers was performed for the same sample amount of ~40 mg in 50 mL of distilled water (at room temperature). Here, the nanofibers were placed into glass beakers and then distilled water was poured to the samples, separately. While each system was shaken (200 rpm) on the incubator, 0.5 mL of test solution was withdrawn, and fresh liquid medium was re-added to these solutions at the pre-determined time intervals. The UV–Vis-spectroscopy measurements were performed for the withdrawn aliquots (250 nm) to determine the released acyclovir amount from nanofibers of acyclovir/HP-βCD and acyclovir/PVP. The calibration curve of acyclovir in water indicated acceptability/linearity with $R^2 \geq 0.99$, and the absorbance intensity values were converted into concentration (μg/mg; released drug molecule amount per unit sample amount) using this calibration curve. The tests were carried out three times (mean values ± standard deviations). The release kinetic of samples were also evaluated using different kinetic models (see supporting information).

2.7. Disintegration test

For the disintegration profiles of acyclovir/HP-βCD and acyclovir/PVP nanofibers, the artificial saliva was prepared to simulate the physicochemical environment of tongue [64]. Here, filter paper was positioned into a plastic petri dish (10 cm), then it was wetted with artificial saliva (10 mL). Artificial saliva was prepared by mixing 2.38 g Na_2HPO_4, 0.190 g KH_2PO_4 and 8 g NaCl in 1 L distilled water and further adjusting its pH to 6.8 with phosphoric acid. After filter paper got wetted, the extra artificial medium was drained from the petri dish. Then, nanofibrous webs having dimensions of ~2.5 cm × 3.8 cm was left onto the filter paper and a video was filmed simultaneously (Video S1).

2.8. Statistical analyses

The statistical analyses were conducted using the one-way/two-way of variance (ANOVA). OriginLab (Origin 2020, USA) was used for all these ANOVA analyses (0.05 level of probability).

3. Results and discussion

3.1. Phase solubility analysis

In this study, the phase solubility analysis has been performed to observe the effect of increasing CD concentration on the solubility of acyclovir molecules [63,65]. Fig. 2 depicts the phase solubility diagram plotted using the UV–Vis measurements results. The phase solubility profile followed in the range of 0–40 mM HP-βCD concentration has not indicated a distinct difference in terms of solvated acyclovir amount. Therefore, the phase solubility diagram has been plotted for the HP-βCD concentration from 40 mM to 160 mM. The linear increase of the acyclovir concentration against the increasing HP-βCD concentrations has identified the A_L type phase solubility diagram which is interpreted as the complex formation with 1/1 (drug/CD) molar ratio [63]. It has been also reported in the previous studies that acyclovir tends to form 1/1 inclusion complex with both HP-βCD [45,66] and βCD [48,49]. Here, the water solubility of acyclovir has been determined as ~2.5 mM in the absence of HP-βCD and it has increased by ~1.5 times with the highest HP-βCD concentration of 160 mM. The binding constant (K_s) of acyclovir/HP-βCD system has been calculated as ~2.5 M^{-1} for the given experimental conditions. Our finding is approximately similar with the study of Saxena et al. in which the K_s value of acyclovir/HP-βCD system was determined as ~11 M^{-1} [66]. In the other related studies, the Ks value have been reported as 8 M^{-1} [67] and 22 M^{-1} [49] for tricyclic acyclovir/HP-βCD and acyclovir/βCD systems, respectively. On the other hand, Nair et al. has reported this value to be ~276 M^{-1} for the HP-βCD concentration range of 0–10 mM [45]. However, as we discussed, we could not observe a significant change for the concentration of acyclovir in this given HP-βCD concentration range. As Loftsson et al. reported, this variation might be due to the different substitution degree (SD) of hydroxypropyl groups in HP-βCD which can result in different binding strength between CD and drug molecules [68].

3.2. Visualization of nanofibers

As it has been conveyed in the previous studies, acyclovir tends to form 1/1 (molar ratio, drug/CD) inclusion complexes with HP-βCD in a way that hydroxyl ethoxy methyl group of acyclovir molecule is encapsulated into the apolar cavity of HP-βCD, while the purine unit gets position through the wider rim of the CD molecule (Fig. 1) [45,47]. Depending on both our phase solubility result and the other reported studies, we have initially prepared the acyclovir/HP-βCD aqueous system with 1/1 M ratio. Unfortunately, the ultimate system was distinctively turbid and heterogenous for the electrospinning of the free-standing nanofibrous webs. Here, the highly concentrated HP-βCD solutions (180%, *w/v*) was used for the electrospinning which is essential to obtain homogenous nanofibers from CDs [69]. However, this highly viscous solutions of HP-βCD has inhibited the effectual mixing of acyclovir/HP-βCD (1/1) system to attain 1/1 complexation and substantial electrospinning yield. Therefore, the content of acyclovir has been decreased and the acyclovir/HP-βCD aqueous system having molar ratio of 1/2 (drug/CD) was prepared for the electrospinning of acyclovir/HP-βCD nanofibrous webs. It has been found that the acyclovir/HP-βCD (1/2) system was quite feasible to form nanofibrous webs effectively. The acyclovir content of the acyclovir/HP-βCD (1/2) nanofibers has corresponded to the 7% (*w*/w, with respect to whole sample amount), so the control sample of acyclovir/PVP nanofibers was prepared so as to include the same amount of acyclovir (7% (*w*/w)) in the ultimate web structure. Differently from acyclovir/HP-βCD aqueous system, ethanol/water (3/1, *v*/v) solvent blend has been used for the electrospinning of acyclovir/PVP nanofibers. As it was depicted in Fig. 3, both acyclovir/HP-βCD and acyclovir/PVP systems have been successfully electrospun into free-standing and flexible nanofibrous webs. It is noteworthy that, both acyclovir/HP-βCD and acyclovir/PVP solution system have had a turbid feature which indicated the existence of uncomplexed/crystal drug parts in the systems (Fig. 3b–d).

The SEM results indicated that the HP-βCD, acyclovir/HP-βCD, PVP and acyclovir/PVP nanofibers have been obtained with homogeneous and defect-free morphology (Fig. 3). The average diameter (AD) of the electrospun nanofibers and the solution properties of conductivity and viscosity of each system were summarized in Table 1. It is a fundamental phenomenon of the electrospinning technique that the stretching process on the solution jet becomes more influential in case of higher conductivity and lower viscosity of the solution and this results in thinner fiber formation [70,71]. Here, AD of the pristine HP-βCD and acyclovir/HP-βCD nanofibers were determined as 505 ± 160 nm and 370 ± 150 nm, respectively. Since acyclovir/HP-βCD nanofibers have been obtained with the lower HP-βCD concentration (180%, *w/v*) than pristine HP-βCD nanofibers (200%, w/v), acyclovir/HP-βCD system has lower viscosity and higher conductivity compared to HP-βCD system (Table 1) [69]. Therefore, the electrospinning jet of acyclovir/HP-βCD has been exposed to higher stretching effect during process and thinner fibers were obtained compared to pristine HP-βCD system. On the other hand, PVP and acyclovir/PVP nanofibers have been obtained having the AD values of 1090 ± 210 nm and 985 ± 385 nm, respectively. As it is seen in Table 1, there is no distinct difference between the solution properties (conductivity and viscosity) of PVP and acyclovir/PVP and this has explained the similarity between the AD values of these two samples. The morphological properties of electrospun nanofibers also depend on further parameters such as polarity, surface tension, composition of the solvent, the polymer types *etc*. [71]. Here, the control samples have been produced using a carrier matrix of PVP in ethanol/water (3/1, *v*/v) blend system, whereas water has been used for HP-βCD based systems. In other words, there might be further parameters apart from the viscosity and conductivity which can have effect on the morphology of these two different systems.

3.3. ^{1}H NMR analysis and the loading efficiency test

Here, the structural examination of acyclovir/HP-βCD and acyclovir/PVP nanofibers has been performed using ^{1}H NMR technique. The characteristic peaks of acyclovir observed in the ^{1}H NMR spectra of electrospun samples has confirmed the loading of this drug molecule into the nanofibrous webs of acyclovir/HP-βCD and acyclovir/PVP (Fig. 4). It is also clear that the acyclovir peaks in the ^{1}H NMR spectra of acyclovir/HP-βCD and acyclovir/PVP nanofibers have the same feature with the acyclovir powder which reveals the structural preservation of this drug molecule throughout the preparation and electrospinning steps. ^{1}H NMR results might also be utilized for the quantitative calculations of each component present in the sample. For this, all samples have been dissolved in *d6*-DMSO prior the measurements to ensure the complete dissolution of whole components in the solution. For both electrospun nanofibers, the proton peaks of acyclovir which located at ~5–11 ppm [45] and did not overlap with the peaks of HP-βCD or PVP have been used for the calculations. On the other hand, the $-CH_3$ peak of HP-βCD at 1.03 ppm [72] and the $-CH_2$ peaks of PVP between 1.2 and 2.4 ppm [73] have been utilized for the calculations. Here, the integrated areas of the predetermined peaks have been proportioned to each other to detect the approximate acyclovir content in the nanofibers of acyclovir/HP-βCD and acyclovir/PVP. Both nanofibrous webs have been prepared so as to include the ~7% (*w*/w, according to total sample) acyclovir in the samples. The ^{1}H NMR findings have indicated that acyclovir/HP-βCD and acyclovir/PVP nanofibers have been obtained with an approximate loading capacity of 7.0% (*w*/w) and 4.7% (w/w) which corresponded to the ~100% and ~ 67% loading efficiency, respectively. In this study, the loading efficiency of nanofibrous webs have been further examined precisely by dissolving samples in DMSO. It was observed that, acyclovir/HP-βCD and acyclovir/PVP nanofibers have been obtained having the loading efficiency of 97.9 ± 2.4% and 66.4 ± 0.7% which corresponds to the loading capacity of 6.85 ± 0.17% (w/w) and 4.65 ± 0.05% (w/w), respectively. These findings are approximate to the ^{1}H NMR results in which the loading capacity of acyclovir has been determined to be ~7.0% and ~ 4.7% for acyclovir/HP-βCD nanofibers and acyclovir/PVP nanofibers, respectively. The ^{1}H NMR and loading efficiency test results have been summarized in Table S1. As it is seen, acyclovir/HP-βCD nanofibers have been obtained with a higher loading efficiency compared to acyclovir/PVP nanofibers. This is most probably due to the inclusion complex formation between acyclovir and HP-βCD in the sample which may provide a better encapsulation efficiency for drug molecule of acyclovir during the preparation and electrospinning processes. As it will be also addressed in the following sections, there have been uncomplexed/crystal acyclovir parts in acyclovir/HP-βCD and acyclovir/PVP nanofibers, however the ^{1}H NMR solvent of *d6*-DMSO and DMSO used for loading efficiency test has dissolved both complexed/uncomplexed and amorph/crystal acyclovir parts exist in the structure of nanofibrous samples. It is noteworthy that, the statistical analyses demonstrated the significant variation between samples ($p < 0.05$).

3.4. Physical state of components and thermal profiles

The physical state of components in the nanofibrous web samples has been evaluated using X-ray diffraction (XRD) and differential scanning calorimetry (DSC) techniques (Fig. 5). Acyclovir is a crystalline material which has been clearly proven by the endothermic peak (258 °C) observed at the DSC thermograms and the numerous diffraction peaks (2θ = 7.1°, 10.6°, 16.1°, 23.9°, 26.2°, 29.4°) present at the XRD graph of the acyclovir powder. As reported by Lutker et al., acyclovir can be in the form of un-hydrated or hydrated crystals [74]. According to this previous report, XRD pattern which we have obtained is coherent with the commercial acyclovir form that has 3:2 acyclovir/H_2O hydrated crystal type [74]. On the other hand, the diffraction

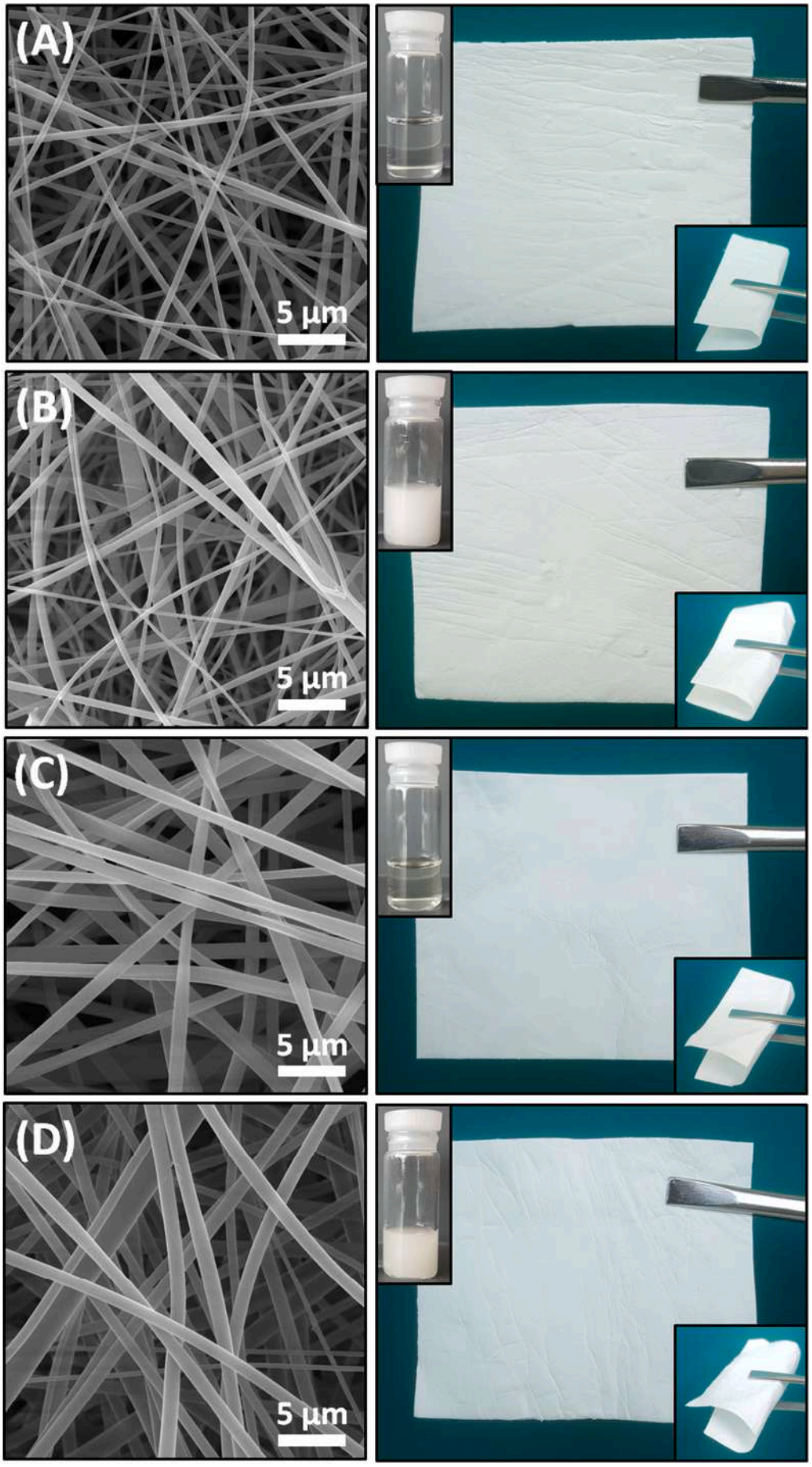

(caption on next page)

Fig. 3. The representative SEM images, the photos of electrospinning solutions and the ultimate electrospun nanofibrous webs of (A) HP-βCD, (B) acyclovir/HP-βCD, (C) PVP and (D) acyclovir/PVP systems.

pattern with two broad haloes indicating that both HP-βCD and PVP has exhibited amorphous structure (Fig. 5A) [69,75]. Since HP-βCD and PVP are amorphous, their DSC thermograms also has not showed a sharp endothermic peak in accordance with the melting point. However, there were respectively, endothermic transition having maximum at ~76 °C and ~ 90 °C in the DSC graphs of pure HP-βCD and PVP nanofibers related to dehydration process (Fig. 5B). As it has been discussed previously, the acyclovir solutions prepared with both HP-βCD and PVP have turbid feature suggesting the existence of uncomplexed/crystal acyclovir in the systems. Therefore, it is probable to encounter with acyclovir crystals in case of ultimate electrospun nanofibrous webs, as well.

Fundamentally, the drug compound incorporated into electrospun nanofibers may exhibit amorphous property due to the fast evaporation of solvent during the electrospinning process. However, this situation generally requires the use of organic solvent to completely dissolve the drug molecules and disturb their crystal structure in the electrospinning solutions prior the process. In our case, the acyclovir powder has just dispersed in the ethanol/water (3/1, *v*/v) solvent system without dissolving which has been used for the electrospinning of acyclovir/PVP nanofibers. Because acyclovir has very limited solubility in water (~ 1.1 mg/mL) and it is almost non-soluble in alcohols [76]. As expected, the characteristic peaks of acyclovir have been prominently observed in the XRD graphs of acyclovir/PVP nanofibrous webs (Fig. 5A-ii). This finding has verified the dispersion of acyclovir crystals within the sample. For acyclovir/HP-βCD nanofibers, water has been used for the dispersion of acyclovir in the HP-βCD solution and for the further inclusion complex formation between acyclovir and HP-βCD. It has been reported in the previous studies that, the crystalline drug molecules can be converted into amorphous status in the CD inclusion complex nanofibers [36,39,40]. This is due to the encapsulation of drug molecules into the CD cavity which can inhibit the further packing of drug molecules into crystal structure again, during or after the electrospinning process. However, we have observed the characteristic diffraction peaks of acyclovir in acyclovir/HP-βCD nanofibers which has indicated the uncomplexed acyclovir parts in the nanofibrous webs. It is also obvious that while the broad diffraction pattern of PVP has been distinctly dominated by the crystal peaks of acyclovir in case of acyclovir/PVP nanofibers, the amorphous XRD profile of HP-βCD having two haloes was still distinctly apparent for acyclovir/HP-βCD nanofibers with less intense acyclovir peaks compared to PVP based sample. This is most probably the result of the inclusion complex formation between HP-βCD and acyclovir in acyclovir/HP-βCD nanofibrous webs. Hence, less amount of acyclovir has remained in crystal state in this sample whereas the huge amount of acyclovir has been in crystal form in case of PVP nanofibers. For more clear evaluation, the XRD graphs of acyclovir/HP-βCD and acyclovir/PVP nanofibers have been curve fitted using Lorentzian distribution and the integrated areas have been used to determine the approximate crystal ratio through the electrospun nanowebs. It has been found that acyclovir/PVP nanofibers had higher crystallinity ratio of 7.4%, while acyclovir/HP-βCD nanofibers had ~4.2%. Even though, both nanofibrous webs contain acyclovir crystals, they have not been detected in SEM images (Fig. 3). This might be due to the homogenous distribution of acyclovir as small crystals within the nanofibrous webs. Additionally, the crystal pattern of both acyclovir/HP-βCD and acyclovir/PVP nanofibers have been checked after 8 months of storage (50–70% RH and at ~20–22 °C) (Fig. S1). It has been detected that, there has been almost no increase or differentiation in the crystal peaks of acyclovir in case of acyclovir/HP-βCD nanofibers. This revealed that HP-βCD platform has ensured an effective preservation and stability for acyclovir during the long-term storage without a potential re-crystallization. On the other hand, we have detected differences at the XRD graph of acyclovir/PVP nanofibers where the crystal peaks of acyclovir were coherent with another hydrated crystal types of acyclovir having 2:1 acyclovir/H_2O ratio [74]. This finding demonstrated that acyclovir/PVP nanofibers may not protect the initial state of the acyclovir and can lead to differentiation of crystal forms during the long-term storage differently from acyclovir/HP-βCD nanofibers.

On the other hand, the alteration in the DSC graphs such as disappearance, broadening, or shift of the melting, decomposition, or oxidation peaks can be referred for examining the interaction between components in the samples [77,78]. Here, the distinct melting peak of acyclovir has not been detected for neither acyclovir/HP-βCD nor acyclovir/PVP nanofibers (Fig. 5B). However, for both acyclovir/HP-βCD and acyclovir/PVP nanofibers, there have been small and broad endothermic peak at about 235 °C differently from their pristine form and this is most probably correlated with the acyclovir crystals present in the samples (Fig. 5B). The incorporation of drug molecule has also induced differentiations in the dehydration profile of HP-βCD and PVP. In case of inclusion complexation, the total enthalpy change (ΔH in J/g) value of CD molecule can be lower compared to its pristine form due to the replacement of guest molecules with the water molecules in the cavity [79]. Even the hydrated type of acyclovir has been used, the value of dehydration ΔH has decreased from ~162 J/g to 148 J/g for acyclovir/HP-βCD reflecting the complex formation between acyclovir and HP-βCD and the dissipation of the acyclovir crystals [72,77]. For acyclovir/PVP nanofibers, the ΔH value has been determined as 262 J/g and 292 J/g for PVP and acyclovir/PVP nanofibers, respectively. Here, the increase of ΔH value might depend on hydrated crystal form of acyclovir which has been incorporated into PVP nanofibers [74]. For this reason, higher amount of water molecule might be held in the composition of acyclovir/PVP nanofibers and this might require using higher energy for the dehydration process.

Additionally, the thermal gravimetric analyzer (TGA) has been used to get information about the thermal degradation profiles of acyclovir powder, pristine HP-βCD and PVP nanofibers, acyclovir/HP-βCD and acyclovir/PVP nanofibers. Fig. 6 showed the TGA thermograms of each sample. Acyclovir powder has displayed three main weight loss steps between 40 °C and 530 °C. As it has been discussed previously, the commercial acyclovir used in this study has the hydrated crystal form of 3:2 acyclovir/H_2O [74,80]. Therefore, the initial step at 40–180 °C was due to the loss of water molecules in the hydrated crystals of acyclovir powder. The second weight loss at 293 °C has corresponded to the decay of hydroxyl ethoxy methyl side chain from the purine unit which further has degraded as third step at 478 °C [74,81]. The TGA

Table 1
The solution properties and the fiber diameters of resulting electrospun nanofibers.

Sample	Solvent	Concentration (%, *w/v*)	Viscosity (Pa·s)	Conductivity (μS/cm)	Average diameter (nm)
HP-βCD	Water	200	1.968	34.44	505 ± 160
Acyclovir/HP-βCD	Water	180	1.309	43.57	370 ± 150
PVP	Ethanol/water (3/1, v/v)	50	0.984	48.47	1090 ± 210
Acyclovir/PVP	Ethanol/water (3/1, v/v)	50	0.850	48.94	985 ± 385

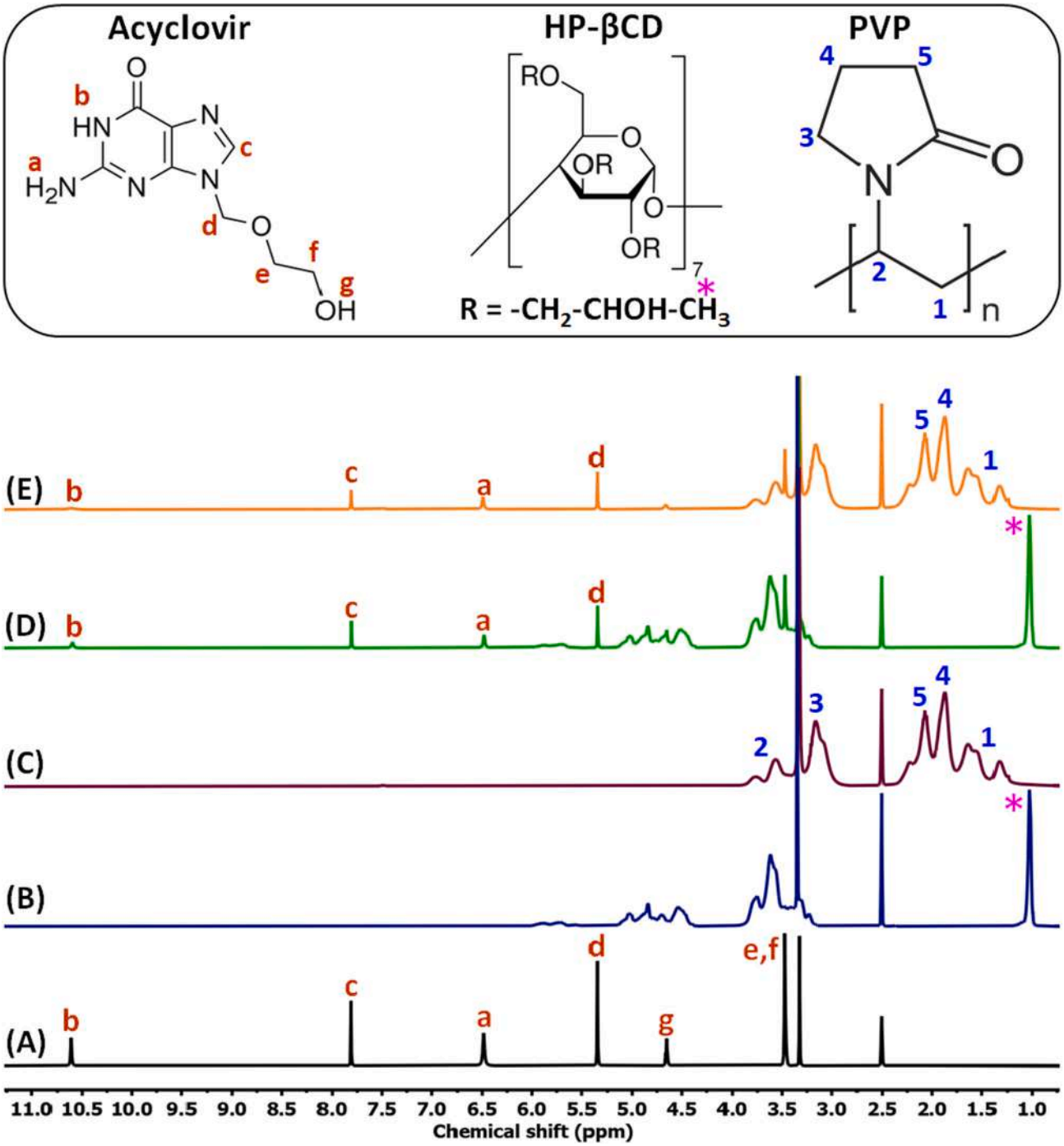

Fig. 4. ^{1}H NMR spectra of (A) acyclovir powder, (B) HP-βCD nanofibers, (C) PVP nanofibers, (D) acyclovir/HP-βCD nanofibers and (E) acyclovir/PVP nanofibers (samples were dissolved in *d6*-DMSO).

thermograms of pristine HP-βCD and PVP nanofibers has exhibited two main weight losses (Fig. 6). The initial weight loss below 100 °C was a result of water evaporation and the second peaks at 358 °C and 439 °C were due to the main degradation of HP-βCD and PVP, respectively. For acyclovir/HP-βCD nanofibers, there have been two weight loss steps due to the water evaporation (below 100 °C) and degradation of HP-βCD (350 °C). As it is seen, the acyclovir degradation has not been detected in the TGA thermogram of acyclovir/HP-βCD nanofibers as a separate step. However, it is obvious in the derivate TGA thermograms that the main degradation step of HP-βCD has shifted to lower temperature value from 358 °C to 350 °C with decreased weight loss ratio (%) compared to pristine HP-βCD (Fig. 6A). This has suggested the incorporation of acyclovir into nanofibrous webs along with an interaction between acyclovir and HP-βCD [82]. Moreover, it has been found from the TGA data that the water content of pristine HP-βCD nanofibers has decreased from ~4.0% to ~2.8% in case of acyclovir/HP-βCD nanofibers. This finding can be also considered as an evidence for the inclusion complex formation between acyclovir and HP-βCD, since water molecules in the cavity of HP-βCD has replaced with the guest molecule of acyclovir and this has resulted in lower water content for acyclovir/HP-βCD nanofibers [79]. In case of acyclovir/PVP nanofibers, the water content of sample has been detected slightly higher (~ 5.0%) compared to pristine PVP nanofibers (~ 4.7%) which has been also found and discussed in DSC analysis. Additionally, there has been

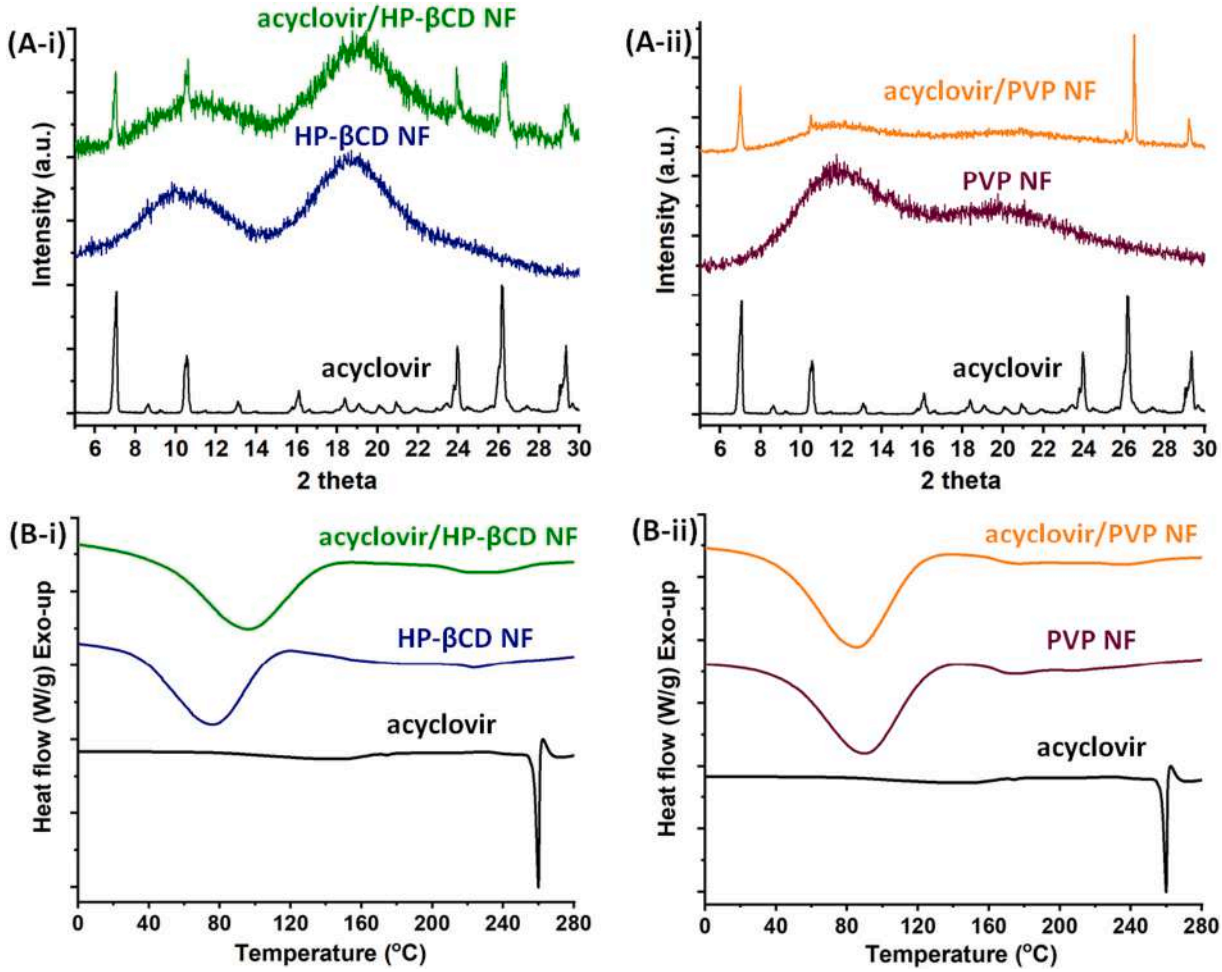

Fig. 5. (A) XRD patterns and (B) DSC thermograms of (i) acyclovir powder, HP-βCD nanofibers (NF), acyclovir/HP-βCD nanofibers (NF) and (ii) acyclovir powder, PVP nanofibers (NF), acyclovir/PVP nanofibers (NF).

no detected shift at the main degradation step of PVP (440 °C) in acyclovir/PVP sample compared to pristine PVP one (439 °C) (Fig. 6B). Here, the weight loss ratio (%) of the PVP derivate peak has only decreased and all these findings has demonstrated that the acyclovir has been incorporated into PVP nanofibers by physical blending without an additional interaction.

3.5. In vitro release profile

The *in vitro* release profile of acyclovir/HP-βCD and acyclovir/PVP nanofibers were given in Fig. 7. As it is seen, acyclovir/HP-βCD nanofibers have almost reached the highest released concentration of 66.4 ± 7.2 μg/mg in 30 s and then approximately plateau profile has been observed up to 1 h with a very slight increase (70.0 ± 0.7 μg/mg). A similar result has been also observed in our previous study where the CD inclusion complex nanofibers of hydrocortisone released almost all drug molecules in the first 30 s due to its fast-dissolution and fast-release properties [40]. On the other hand, acyclovir/PVP nanofiber has released less amount of acyclovir in 30 s (14.9 ± 0.1 μg/mg) and it has reached to the upper concentration (50.0 ± 2.1 μg/mg) at the end of 1 h (Fig. 7). These results have revealed that both acyclovir/HP-βCD and acyclovir/PVP nanofibers have released ~100% of the loaded acyclovir into the aqueous medium in the given period. On the other hand, both nanofibers have indicated different release profiles. This might be due to both higher solubility of HP-βCD (> 2000 mg/mL) compared to PVP (> 100 mg/mL) and the higher amount of crystalline acyclovir presents in acyclovir/PVP nanofibers. It is worth to mention that acyclovir/HP-βCD nanofibers have readily dissolved by the contact of water medium, while acyclovir/PVP nanofibers have showed slightly slower dissolution in the same medium compared to HP-βCD based system. Due to all these reasons, the release of acyclovir from acyclovir/PVP nanofibers has occurred by gradual dissolution of drug crystals in the aqueous medium at progressing time intervals. Nonetheless, the inclusion complex structure of acyclovir/HP-βCD nanofibers and the interaction between acyclovir and HP-βCD has ensured a distinct improvement for the fast-dissolution profile of acyclovir compared to PVP based system. In one of the related studies, Vigh et al. has also indicated that the solubility/dissolution rate of the hydrophobic drug of spironolactone has increased gradually with the increasing ratio of HP-βCD in the PVP based nanofibrous web formulation [42].

The release test results have also validated the lower acyclovir content of acyclovir/PVP nanofibers compared to acyclovir/HP-βCD nanofibers, since PVP based system released lower amount of acyclovir (50.0 ± 2.1 μg/mg) than HP-βCD one (70.0 ± 0.7 μg/mg). These findings are also correlated with the results of ^{1}H NMR and loading efficiency analyses in which the loading capacities of acyclovir/HP-βCD and acyclovir/PVP nanofibers have been determined as ~7.0% (*w*/w) (corresponds to the ~7 μg/mg) and ~ 4.7% (w/w) (corresponds to the ~4.7 μg/mg), respectively. Here, the significant variations between the samples have been revealed by the statistical analyses ($p < 0.05$). In this study, various kinetic models have been also applied in order to explore the release profiles of samples. The formulations, fitting graphs (Fig. S2) and the R^2 (correlation coefficient) (Table S2) values were reported in supporting information. The R^2 values has demonstrated

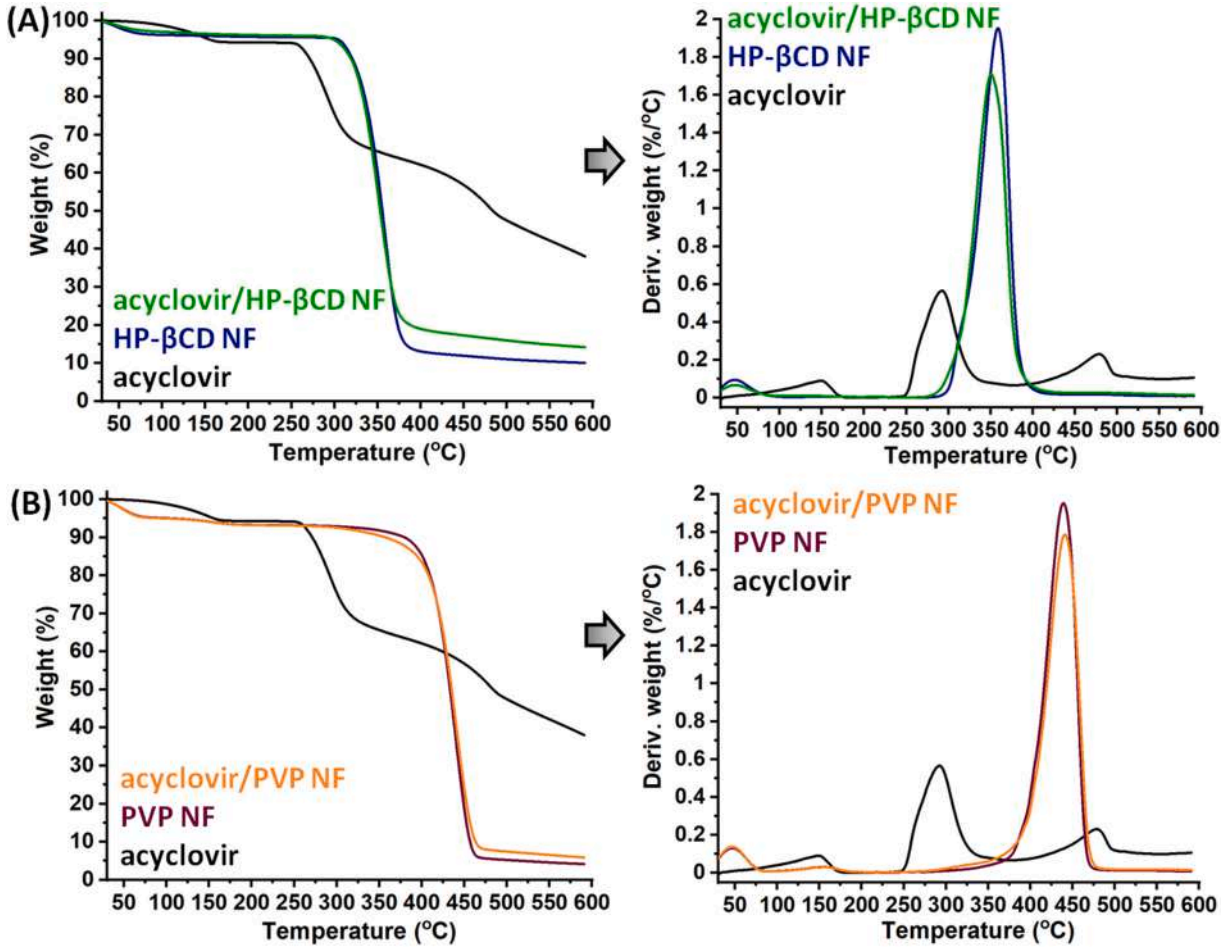

Fig. 6. TGA thermograms and derivates of (A) acyclovir powder, HP-βCD nanofibers (NF), acyclovir/HP-βCD nanofibers (NF) and (B) acyclovir powder, PVP nanofibers (NF), acyclovir/PVP nanofibers (NF).

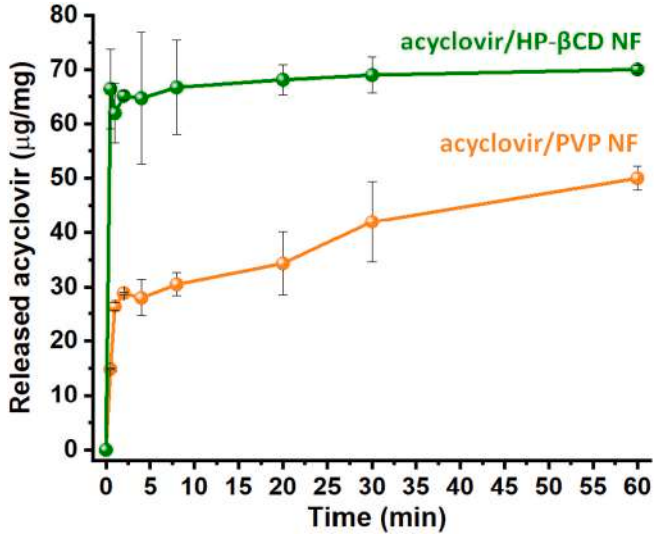

Fig. 7. Time dependent release profiles acyclovir/HP-βCD nanofibers and acyclovir/PVP nanofibers.

that the release behavior of acyclovir/HP-βCD nanofibers was not compatible with the given kinetic models of zero/first order and Higuchi. This has exhibited that the release of acyclovir from acyclovir/HP-βCD nanofibers has not depended on time and not raised from a planar matrix that is insoluble in water (Fick's first law) [83]. However, acyclovir/HP-βCD nanofibers has showed the relatively highest coherence with the Korsmeyer–Peppas model among others and the diffusion exponent (n) value has been found in the $0.45 < n < 0.89$ range. This finding might be interpreted for the non-Fickian or irregular diffusion of acyclovir from the acyclovir/HP-βCD nanofibers by diffusion-based and erosion-controlled release [83,84].

On the contrary, acyclovir/PVP nanofibers have shown better fitting with each of these given kinetic models compared to acyclovir/HP-βCD nanofibers. It has been found that the acyclovir/PVP nanofibers have highest consistency with first-order kinetics ($R^2 = 0.9303$) and this has suggested that the acyclovir was prone to be released in a time-dependent way in case of acyclovir/PVP nanofibers [83]. As in acyclovir/HP-βCD nanofibers, the diffusion exponent (n) value of acyclovir/PVP nanofibers has also been determined in the range of $0.45 < n < 0.89$. This has also presented the erosion-controlled and diffusion-based release of acyclovir from acyclovir/PVP nanofibers [83,84]. The disintegration profile of acyclovir/HP-βCD and acyclovir/PVP nanofibers have been also evaluated in the artificial saliva environment which was created using wetted filter paper. The photos captured from the Video S1 was given in Fig. 8. It is obvious that, acyclovir/HP-βCD has instantly disappeared in less than 3 s by being absorbed in the artificial saliva. On the other hand, acyclovir/PVP nanofibers have disintegrated in slower manner than acyclovir/HP-βCD nanofibers because of the higher content of crystalline acyclovir and the relatively lower dissolution profile of PVP system compared to HP-βCD one. The faster disintegration profile of acyclovir/HP-βCD nanofibers might make this system more favorable for the oral fast-dissolving dosage formulation compared the polymer-based systems by eliminating the unpleasant

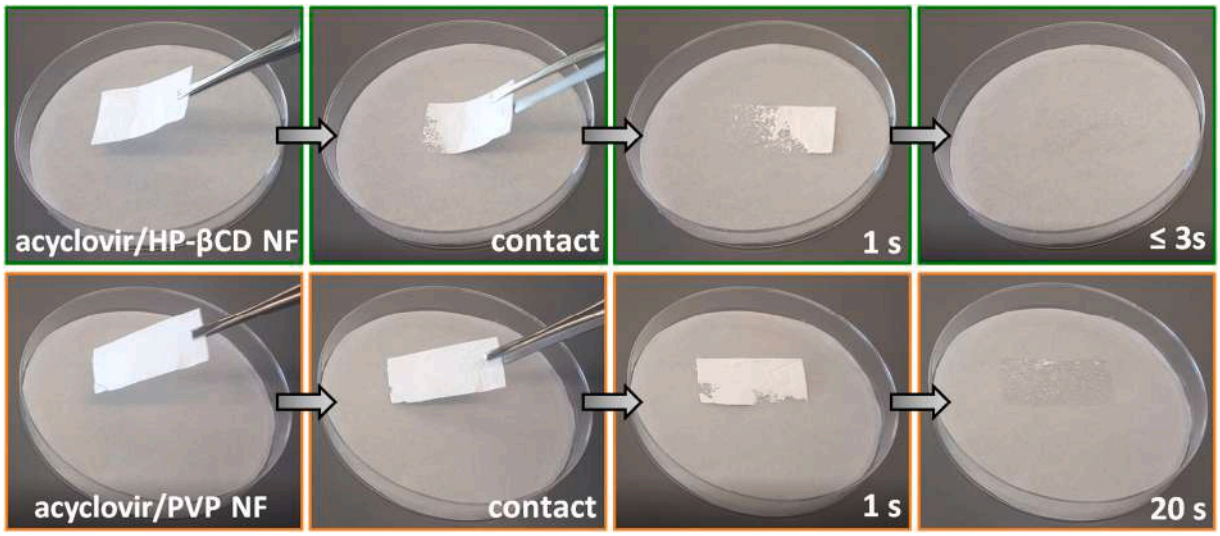

Fig. 8. The disintegration behavior of acyclovir/HP-βCD nanofibers (NF) and acyclovir/PVP nanofibers (NF) at the artificial saliva environment. (Video S1 has been used to capture the photos).

grainy feeling which can occur during the administration.

Besides the water soluble and hydrophilic nature of HP-βCD or PVP, the porous 3D continuous structure and the high surface area of nanofibrous webs are the other main driving forces for the instant dissolving of samples. Because, these features provide effectual penetration ways for the dissolution medium, by increasing the potential contact sides through the nanofibers. Apart from these properties, there are further gains obtained by using HP-βCD as carrier matrix for the fast-dissolving and fast-release properties of nanofibrous webs. For instance, the significantly high water solubility of HP-βCD (> 2000 mg/mL) and the inclusion complexation property which can ensure the amorphous distribution of drug molecules. Briefly, the inclusion complexation between acyclovir and HP-βCD and significantly high water solubility of HP-βCD have created difference and ensured the fast-dissolution rate and so the release of acyclovir differently from acyclovir/PVP nanofibers and faster disintegration profile in saliva simulation. Therefore, acyclovir/HP-βCD nanofibers might be an attractive alternative as a fast-dissolving oral drug delivery system counter to common polymeric dosage formulations.

4. Conclusion

In this report, the polymer free acyclovir/hydroxypropyl-beta-cyclodextrin (HP-βCD) nanofibers have been successfully generated with uniform morphology and free-standing feature. As a control sample, polymeric nanofibrous webs of acyclovir/polyvinylpyrrolidone (PVP) have been fabricated, as well. The ultimate nanofiber of acyclovir/HP-βCD and acyclovir/PVP have been obtained with the loading efficiency of ~98% and ~ 66%, respectively. In comparison with PVP based system, HP-βCD has substantially provided amorphous distribution of acyclovir in the nanofibrous webs by the inclusion complexation. The inclusion complexation, the high water solubility of HP-βCD, highly porous structure and high surface area of nanofibers have ensured the rapid release of this antiviral drug molecule from acyclovir/HP-βCD nanofibers. However, the release of acyclovir in acyclovir/PVP nanofibers has occurred by the gradual dissolution of drug crystals in the aqueous medium. In addition to fast-dissolution and so the immediate release of acyclovir from electrospun nanofibrous mats, acyclovir/HP-βCD nanofibers have also disintegrated more instantly when contact to artificial saliva compared to acyclovir/PVP nanofibers. It is noteworthy to state that, while water has been used in the electrospinning of acyclovir/HP-βCD nanofibers, acyclovir/PVP nanofibers have been obtained using ethanol/water (3/1, *v*/v) solvent system. Therefore, the preparation and the generation of acyclovir/HP-βCD nanofibers in water can be a huge advantage for the industrialization of this new generation drug dosage forms. To conclude, the concept of cyclodextrin inclusion complex nanofibers which are obtained without using an additional polymeric template and toxic solvent system can be implemented for the antiviral drug molecules. Due to the gains of both electrospinning and cyclodextrins, a novel fast-dissolving oral drug delivery system can be developed along with the enhanced physicochemical properties of drug molecules. This approach might be an attractive alternative to the conventional dosage formulation which are generally generated using commercial polymeric system and excipients.

Supplementary data to this article can be found online at https://doi.org/10.1016/j.msec.2020.111514.

CRediT authorship contribution statement

Asli Celebioglu: Conceptualization, Methodology, Validation, Investigation, Writing-Original draft preparation, Writing-Review & Editing. **Tamer Uyar**: Supervision, Resources, Conceptualization, Methodology, Project administration, Funding acquisition.

Declaration of competing interest

The Authors declare that they have no known competing financial interests or personal relationships that could have appeared to influence the work reported in this paper.

Acknowledgments

This work made use of the Cornell Center for Materials Research Shared Facilities which are supported through the NSF MRSEC program (DMR-1719875), and the Cornell Chemistry NMR Facility supported in part by the NSF MRI program (CHE-1531632), and the Department of Fiber Science & Apparel Design facilities. Prof. Uyar acknowledges the startup funding from the College of Human Ecology at Cornell University. The partial funding for this research was also graciously provided by Nixon Family (Lea and John Nixon) thru College of Human Ecology at Cornell University.

References

[1] R. Bala, S. Khanna, P. Pawar, S. Arora, Orally Dissolving Strips: A New Approach to Oral Drug Delivery System, Int. J. Pharm, Investig, 2013, https://doi.org/10.4103/

2230-973x.114897.
[2] H. Kathpalia, A. Gupte, An introduction to fast dissolving Oral thin film drug delivery systems: a review, Curr. Drug Deliv. (2013), https://doi.org/10.2174/15672018100613112515024 9.
[3] V.F. Patel, F. Liu, M.B. Brown, Advances in oral transmucosal drug delivery, J. Control. Release 153 (2011) 106–116.
[4] P.C. Patil, S.K. Shrivastava, S. Vaidehi, P. Ashwini, Oral fast dissolving drug delivery system: a modern approach for patient compliance, Int. J. Drug Regul. Aff. 2 (2014) 49–60.
[5] R.D. Rahane, P.R. Rachh, A review on fast dissolving tablet, J. Drug Deliv. Ther. 8 (2018) 50–55.
[6] M. Ciper, R. Bodmeier, Preparation and characterization of novel fast disintegrating capsules (Fastcaps) for administration in the oral cavity, Int. J. Pharm. 303 (2005) 62–71.
[7] S. Seif, L. Franzen, M. Windbergs, Overcoming drug crystallization in electrospun fibers–elucidating key parameters and developing strategies for drug delivery, Int. J. Pharm. 478 (2015) 390–397.
[8] D.-G. Yu, J.-J. Li, G.R. Williams, M. Zhao, Electrospun amorphous solid dispersions of poorly water-soluble drugs: a review, J. Control. Release 292 (2018) 91–110.
[9] T. Uyar, E. Kny, Electrospun Materials for Tissue Engineering and Biomedical Applications: Research, Design and Commercialization, Woodhead Publishing, 2017.
[10] K. Wang, P. Wang, M. Wang, D.-G. Yu, F. Wan, S.W.A. Bligh, Comparative study of electrospun crystal-based and composite-based drug nano depots, Mater. Sci. Eng. C. 110988 (2020).
[11] Y. Yang, B. Xie, Q. Liu, B. Kong, H. Wang, Fabrication and characterization of a novel polysaccharide based composite nanofiber films with tunable physical properties, Carbohydr. Polym. 236 (2020) 116054.
[12] J. Yang, K. Wang, D.-G. Yu, Y. Yang, S.W.A. Bligh, G.R. Williams, Electrospun Janus nanofibers loaded with a drug and inorganic nanoparticles as an effective antibacterial wound dressing, Mater. Sci. Eng. C. 110805 (2020).
[13] S. Chang, M. Wang, F. Zhang, Y. Liu, X. Liu, D.-G. Yu, H. Shen, Sheath-separate-core nanocomposites fabricated using a trifluid electrospinning, Mater. Des. 108782 (2020).
[14] E. Sipos, N. Kósa, A. Kazsoki, Z.-I. Szabó, R. Zelkó, Formulation and characterization of aceclofenac-loaded nanofiber based orally dissolving webs, Pharmaceutics. 11 (2019) 417.
[15] S. Tort, A. Yıldız, F. Tuğcu-Demiröz, G. Akca, Ö. Kuzukıran, F. Acartürk, Development and characterization of rapid dissolving ornidazole loaded PVP electrospun fibers, Pharm. Dev. Technol. 24 (2019) 864–873.
[16] H. Bukhary, G.R. Williams, M. Orlu, Electrospun fixed dose formulations of amlodipine besylate and valsartan, Int. J. Pharm. 549 (2018) 446–455.
[17] S. Nam, S.Y. Lee, H.-J. Cho, Phloretin-loaded fast dissolving nanofibers for the locoregional therapy of oral squamous cell carcinoma, J. Colloid Interface Sci. 508 (2017) 112–120.
[18] S. Thakkar, N. More, D. Sharma, G. Kapusetti, K. Kalia, M. Misra, Fast dissolving electrospun polymeric films of anti-diabetic drug repaglinide: formulation and evaluation, Drug Dev. Ind. Pharm. 45 (2019) 1921–1930.
[19] A. Akhgari, D.A. Ghalambor, M. Rezaei, M. Kiarsi, M.R. Abbaspour, The Design and Evaluation of a Fast-dissolving Drug Delivery System for Loratadine Using the Electrospinning Method, (2016).
[20] J. Chen, X. Wang, W. Zhang, S. Yu, J. Fan, B. Cheng, X. Yang, W. Pan, A novel application of electrospinning technique in sublingual membrane: characterization, permeation and in vivo study, Drug Dev. Ind. Pharm. 42 (2016) 1365–1374.
[21] U.E. Illangakoon, T. Nazir, G.R. Williams, N.P. Chatterton, Mebeverine-loaded electrospun nanofibers: physicochemical characterization and dissolution studies, J. Pharm. Sci. 103 (2014) 283–292.
[22] F. Mano, M. Martins, I. Sá-Nogueira, S. Barreiros, J.P. Borges, R.L. Reis, A.R.C. Duarte, A. Paiva, Production of electrospun fast-dissolving drug delivery systems with therapeutic eutectic systems encapsulated in gelatin, AAPS PharmSciTech 18 (2017) 2579–2585.
[23] P.S. Giram, A. Shitole, S.S. Nande, N. Sharma, B. Garnaik, Fast dissolving moxifloxacin hydrochloride antibiotic drug from electrospun Eudragit L-100 nonwoven nanofibrous Mats, Mater. Sci. Eng. C. 92 (2018) 526–539.
[24] M. Teodorescu, M. Bercea, S. Morariu, Biomaterials of PVA and PVP in medical and pharmaceutical applications: perspectives and challenges, Biotechnol. Adv. 37 (2019) 109–131.
[25] K. Halake, M. Birajdar, B.S. Kim, H. Bae, C. Lee, Y.J. Kim, S. Kim, H.J. Kim, S. Ahn, S.Y. An, Recent application developments of water-soluble synthetic polymers, J. Ind. Eng. Chem. 20 (2014) 3913–3918.
[26] E. Bilensoy, Cyclodextrins in Pharmaceutics, Cosmetics, and Biomedicine: Current and Future Industrial Applications, John Wiley & Sons, 2011.
[27] S. Kalepu, V. Nekkanti, Insoluble drug delivery strategies: review of recent advances and business prospects, Acta Pharm. Sin. B 5 (2015) 442–453.
[28] M. Pooresmaeil, H. Namazi, R. Salehi, Synthesis of photoluminescent glycodendrimer with terminal β-cyclodextrin molecules as a biocompatible pH-sensitive carrier for doxorubicin delivery, Carbohydr. Polym. 116658 (2020).
[29] M. Pooresmaeil, H. Namazi, Surface modification of graphene oxide with stimuli-responsive polymer brush containing β-cyclodextrin as a pendant group: preparation, characterization, and evaluation as controlled drug delivery agent, Colloids Surfaces B Biointerfaces. 172 (2018) 17–25.
[30] M. Pooresmaeil, H. Namazi, β-Cyclodextrin grafted magnetic graphene oxide applicable as cancer drug delivery agent: synthesis and characterization, Mater. Chem. Phys. 218 (2018) 62–69.
[31] S.B. Carneiro, C. Duarte, F. Ílary, L. Heimfarth, S. Quintans, J. de Souza, L.J. Quintans-Júnior, V.F. da Veiga Júnior, Á.A. Neves de Lima, Cyclodextrin–drug inclusion complexes: in vivo and in vitro approaches, Int. J. Mol. Sci. 20 (2019) 642.
[32] F. Topuz, T. Uyar, Electrospinning of cyclodextrin functional nanofibers for drug delivery applications, Pharmaceutics. 11 (2019) 6.
[33] E. Borbás, A. Balogh, K. Bocz, J. Müller, É. Kiserdei, T. Vigh, B. Sinkó, A. Marosi, A. Halász, Z. Dohányos, In vitro dissolution–permeation evaluation of an electrospun cyclodextrin-based formulation of aripiprazole using μFlux™, Int. J. Pharm. 491 (2015) 180–189.
[34] Z. Aytac, S. Ipek, I. Erol, E. Durgun, T. Uyar, Fast-dissolving electrospun gelatin nanofibers encapsulating ciprofloxacin/cyclodextrin inclusion complex, Colloids Surfaces B Biointerfaces. 178 (2019) 129–136.
[35] Z.I. Yildiz, A. Celebioglu, T. Uyar, Polymer-free electrospun nanofibers from sulfobutyl ether7-beta-cyclodextrin (SBE7-β-CD) inclusion complex with sulfisoxazole: fast-dissolving and enhanced water-solubility of sulfisoxazole, Int. J. Pharm. 531 (2017) 550–558.
[36] A. Celebioglu, T. Uyar, Metronidazole/hydroxypropyl-β-cyclodextrin inclusion complex nanofibrous webs as fast-dissolving oral drug delivery system, Int. J. Pharm. 118828 (2019).
[37] Z.I. Yıldız, T. Uyar, Fast-dissolving electrospun nanofibrous films of paracetamol/cyclodextrin-inclusion complexes, Appl. Surf. Sci. 492 (2019) 626–633.
[38] A. Balogh, T. Horváthová, Z. Fülöp, T. Loftsson, A.H. Harasztos, G. Marosi, Z.K. Nagy, Electroblowing and electrospinning of fibrous diclofenac sodium-cyclodextrin complex-based reconstitution injection, J. Drug Deliv. Sci. Technol. 26 (2015) 28–34.
[39] A. Celebioglu, T. Uyar, Fast dissolving oral drug delivery system based on electrospun nanofibrous webs of cyclodextrin/ibuprofen inclusion complex nanofibers, Mol. Pharm. 16 (2019) 4387–4398.
[40] A. Celebioglu, T. Uyar, Hydrocortisone/Cyclodextrin Complex Electrospun Nanofibers for a Fast-Dissolving Oral Drug Delivery System, RSC Med, Chem, 2020.
[41] P. Vass, B. Démuth, A. Farkas, E. Hirsch, E. Szabó, B. Nagy, S.K. Andersen, T. Vigh, G. Verreck, I. Csontos, Continuous alternative to freeze drying: manufacturing of cyclodextrin-based reconstitution powder from aqueous solution using scaled-up electrospinning, J. Control. Release 298 (2019) 120–127.
[42] T. Vigh, T. Horváthová, A. Balogh, P.L. Sóti, G. Drávavölgyi, Z.K. Nagy, G. Marosi, Polymer-free and polyvinylpirrolidone-based electrospun solid dosage forms for drug dissolution enhancement, Eur. J. Pharm. Sci. 49 (2013) 595–602.
[43] R. Cortesi, E. Esposito, Acyclovir delivery systems, Expert Opin. Drug Deliv. 5 (2008) 1217–1230.
[44] T. Costa, A. Ribeiro, R. Machado, C. Ribeiro, S. Lanceros-Mendez, A.M. Cavaco-Paulo, A. Almeida, J. das Neves, M. Lúcio, T. Viseu, Polymeric electrospun fibrous dressings for topical co-delivery of acyclovir and omega-3 fatty acids, Front. Bioeng. Biotechnol. 7 (2019) 390.
[45] A.B. Nair, M. Attimarad, B.E. Al-Dhubiab, J. Wadhwa, S. Harsha, M. Ahmed, Enhanced oral bioavailability of acyclovir by inclusion complex using hydroxypropyl-β-cyclodextrin, Drug Deliv. 21 (2014) 540–547.
[46] M. Ates, M.S. Kaynak, S. Sahin, Effect of permeability enhancers on paracellular permeability of acyclovir, J. Pharm. Pharmacol. 68 (2016) 781–790.
[47] E. Aicart, E. Junquera, Complex formation between purine derivatives and cyclodextrins: a fluorescence spectroscopy study, J. Incl. Phenom. Macrocycl. Chem. 47 (2003) 161–165.
[48] J. Luengo, T. Aránguiz, J. Sepúlveda, L. Hernández, C. Von Plessing, Preliminary pharmacokinetic study of different preparations of acyclovir with β-cyclodextrin, J. Pharm. Sci. 91 (2002) 2593–2598.
[49] C. von P. Rossel, J. Sepúlveda Carreño, M. Rodríguez-Baeza, J.B. Alderete, Inclusion complex of the antiviral drug acyclovir with cyclodextrin in aqueous solution and in solid phase, Quim. Nova. 23 (2000) 749–752.
[50] M. Koźbiał, P. Gierycz, Comparison of aqueous and 1-octanol solubility as well as liquid–liquid distribution of acyclovir derivatives and their complexes with hydroxypropyl-β-cyclodextrin, J. Solut. Chem. 42 (2013) 866–881.
[51] M. Chavanpatil, P.R. Vavia, Enhancement of nasal absorption of acyclovir via cyclodextrins, J. Incl. Phenom. Macrocycl. Chem. 44 (2002) 137–140.
[52] T. Loftsson, M.E. Brewster, M. Masson, Role of cyclodextrins in improving oral drug delivery, Am. J. Drug Deliv. 2 (2004) 261–275.
[53] T. Loftsson, P. Jarho, M. Masson, T. Järvinen, Cyclodextrins in drug delivery, Expert Opin. Drug Deliv. 2 (2005) 335–351.
[54] D.-H. Kim, S.-E. Lee, Y.-C. Pyo, P. Tran, J.-S. Park, Solubility enhancement and application of cyclodextrins in local drug delivery, J. Pharm. Investig. (2019) 1–11.
[55] M.I. Shekh, J. Amirian, F.J. Stadler, B. Du, Y. Zhu, Oxidized chitosan modified electrospun scaffolds for controllable release of acyclovir, Int. J. Biol. Macromol. 151 (2020) 787–796.
[56] D. Yu, C. Branford-White, L. Li, X. Wu, L. Zhu, The compatibility of acyclovir with polyacrylonitrile in the electrospun drug-loaded nanofibers, J. Appl. Polym. Sci. 117 (2010) 1509–1515.
[57] M. Azizi, M.S. Seyed Dorraji, M.H. Rasoulifard, Influence of structure on release profile of acyclovir loaded polyurethane nanofibers: monolithic and core/shell structures, J. Appl. Polym. Sci. 133 (2016).
[58] Y.-H. Wu, D.-G. Yu, H.-P. Li, X.-Y. Wu, X.-Y. Li, Medicated structural PVP/PEG composites fabricated using coaxial electrospinning, E-Polymers. 17 (2017) 39–44.
[59] J. Wang, M. Windbergs, Influence of polymer composition and drug loading procedure on dual drug release from PLGA: PEG electrospun fibers, Eur. J. Pharm. Sci. 124 (2018) 71–79.
[60] J. Wang, M. Windbergs, Controlled dual drug release by coaxial electrospun fibers–impact of the core fluid on drug encapsulation and release, Int. J. Pharm. 556 (2019) 363–371.
[61] A. Baskakova, S. Awwad, J.Q. Jiménez, H. Gill, O. Novikov, P.T. Khaw, S. Brocchini, E. Zhilyakova, G.R. Williams, Electrospun formulations of acyclovir, ciprofloxacin

and cyanocobalamin for ocular drug delivery, Int. J. Pharm. 502 (2016) 208–218.
[62] S.E. Aniagyei, L.B. Sims, D.A. Malik, K.M. Tyo, K.C. Curry, W. Kim, D.A. Hodge, J. Duan, J.M. Steinbach-Rankins, Evaluation of poly (lactic-co-glycolic acid) and poly (dl-lactide-co-ε-caprolactone) electrospun fibers for the treatment of HSV-2 infection, Mater. Sci. Eng. C. 72 (2017) 238–251.
[63] T. Higuchi, K.A. Connors, Phase solubility diagram, Adv. Anal. Chem. Instrum. 4 (1965) 117–212.
[64] Y. Bi, H. Sunada, Y. Yonezawa, K. Danjo, A. Otsuka, K. IIDA, Preparation and evaluation of a compressed tablet rapidly disintegrating in the oral cavity, Chem. Pharm. Bull. 44 (1996) 2121–2127.
[65] M.E. Brewster, T. Loftsson, Cyclodextrins as pharmaceutical solubilizers, Adv. Drug Deliv. Rev. 59 (2007) 645–666.
[66] A. Saxena, G. Tewari, S.A. Saraf, Formulation and evaluation of mucoadhesive buccal patch of acyclovir utilizing inclusion phenomenon, Brazilian J. Pharm. Sci. 47 (2011) 887–897.
[67] W. Zielenkiewicz, M. Kożbiał, B. Golankiewicz, J. Poznański, Enhancement of aqueous solubility of tricyclic acyclovir derivatives by their complexation with hydroxypropyl-β-cyclodextrin, J. Therm. Anal. Calorim. 101 (2010) 555–560.
[68] T. Loftsson, H. Frikdriksdóttir, A.M. Sigurkdardóttir, H. Ueda, The effect of water-soluble polymers on drug-cyclodextrin complexation, Int. J. Pharm. 110 (1994) 169–177.
[69] A. Celebioglu, T. Uyar, Electrospinning of nanofibers from non-polymeric systems: polymer-free nanofibers from cyclodextrin derivatives, Nanoscale. 4 (2012) 621–631.
[70] T. Uyar, F. Besenbacher, Electrospinning of uniform polystyrene fibers: the effect of solvent conductivity, Polymer (Guildf). 49 (2008) 5336–5343.
[71] J. Xue, T. Wu, Y. Dai, Y. Xia, Electrospinning and electrospun nanofibers: methods, materials, and applications, Chem. Rev. 119 (2019) 5298–5415.
[72] A. Celebioglu, T. Uyar, Development of ferulic acid/cyclodextrin inclusion complex nanofibers for fast-dissolving drug delivery system, Int. J. Pharm. 119395 (2020).
[73] M.I. Loría-Bastarrachea, W. Herrera-Kao, J.V. Cauich-Rodríguez, J.M. Cervantes-Uc, H. Vázquez-Torres, A. Ávila-Ortega, A TG/FTIR study on the thermal degradation of poly (vinyl pyrrolidone), J. Therm. Anal. Calorim. 104 (2011) 737–742.
[74] K.M. Lutker, R. Quiñones, J. Xu, A. Ramamoorthy, A.J. Matzger, Polymorphs and hydrates of acyclovir, J. Pharm. Sci. 100 (2011) 949–963.
[75] D.-G. Yu, J.-M. Yang, C. Branford-White, P. Lu, L. Zhang, L.-M. Zhu, Third generation solid dispersions of ferulic acid in electrospun composite nanofibers, Int. J. Pharm. 400 (2010) 158–164.
[76] R. Cortesi, L. Ravani, E. Menegatti, M. Drechsler, E. Esposito, Colloidal dispersions for the delivery of acyclovir: a comparative study, Indian J. Pharm. Sci. 73 (2011) 687.
[77] P. Mura, Analytical techniques for characterization of cyclodextrin complexes in the solid state: a review, J. Pharm. Biomed. Anal. 113 (2015) 226–238.
[78] G. Wadhwa, S. Kumar, L. Chhabra, S. Mahant, R. Rao, Essential oil–cyclodextrin complexes: an updated review, J. Incl. Phenom. Macrocycl. Chem. 89 (2017) 39–58.
[79] A. Celebioglu, F. Kayaci-Senirmak, S. İpek, E. Durgun, T. Uyar, Polymer-free nanofibers from vanillin/cyclodextrin inclusion complexes: high thermal stability, enhanced solubility and antioxidant property, Food Funct. 7 (2016) 3141–3153.
[80] Y.T. Sohn, S.H. Kim, Polymorphism and pseudopolymorphism of acyclovir, Arch. Pharm. Res. 31 (2008) 231–234.
[81] N.S. Malik, M. Ahmad, M.U. Minhas, Cross-linked β-cyclodextrin and carboxymethyl cellulose hydrogels for controlled drug delivery of acyclovir, PLoS One 12 (2017).
[82] A. Celebioglu, T. Uyar, Fast-dissolving antioxidant curcumin/cyclodextrin inclusion complex electrospun nanofibrous webs, Food Chem. 317 (2020) 126397.
[83] N.A. Peppas, B. Narasimhan, Mathematical models in drug delivery: how modeling has shaped the way we design new drug delivery systems, J. Control. Release 190 (2014) 75–81.
[84] X. Li, M.A. Kanjwal, L. Lin, I.S. Chronakis, Electrospun polyvinyl-alcohol nanofibers as oral fast-dissolving delivery system of caffeine and riboflavin, Colloids Surfaces B Biointerfaces. 103 (2013) 182–188.